Porous Silica Nanocapsules and Nanospheres: Dynamic Self-Assembly Synthesis and Application in Controlled Release

Hongmin Chen,[†,‡] Junhui He,*[,†] Huamin Tang,[§] and Chunxiao Yan[§]

Functional Nanomaterials Laboratory and Key Laboratory of Photochemical Conversion and Optoelectronic Materials, Technical Institute of Physics and Chemistry, Chinese Academy of Sciences (CAS), Beijing 100190, Graduate University of the Chinese Academy of Sciences, Beijing 100049, and Institute of Chemical Defense, Beijing 102205, China

Received May 23, 2008

In this work, porous silica nanocapsules and silica nanospheres have been successfully fabricated by a novel combination of stabilizing condensation and dynamic self-assembly. When ethyl ether was used as a cosolvent, porous silica nanocapsules were obtained. In contrast, when 2-ethoxyethanol was used, silica porous nanospheres were produced. The silica nanostructures were characterized by small-angle X-ray diffraction, scanning electron microscopy, energy dispersive spectroscopy, transmission electron microscopy, and nitrogen adsorption−desorption measurements. They had high Brunauer−Emmett−Teller specific surface areas and large pore volumes. The order of their pore structures increased with an increase of the corresponding cosolvent. In situ encapsulation of organic molecules into silica nanocapsules and their controlled release were further investigated by using pyrene as a typical example. As many dyes, drugs, etc. are organic molecules, the current approaches will doubtlessly open many possibilities toward biological and technological applications.

Introduction

In recent years, the design and fabrication of porous capsules and spheres of well-defined morphologies have attracted much attention because of their low density, large surface area, high permeability, and potential applications in cosmetics, catalysis, coatings, composite materials, dyes, inks, artificial cells, and fillers and as microencapsulates for target molecules.[1−5] These studies may also shed light on fundamental mechanisms of biomineralization.[6] Porous silica nanocapsules and nanospheres are of specific interest as they are promising in nanocasting,[7,8] drug delivery and controlled release,[9−11] and material transport[12,13] and as nanoreactors.[14] Hard templates,[15−17] vesicles,[18,19] emulsions,[20,21] etc. have been employed to prepare porous capsules and spheres. These approaches to fabrication of porous capsules and spheres using sacrificial templates have proven successful. However, synthesis of porous capsules and spheres of well-defined morphologies is still a challenge, and in situ encapsulation of target molecules is still another challenge.

* To whom correspondence should be addressed. Phone/Fax: +86-10-8254 3535. E-mail: jhhe@mail.ipc.ac.cn.
† Technical Institute of Physics and Chemistry, CAS.
‡ Graduate University of the CAS.
§ Institute of Chemical Defense.

(1) (a) Pouget, E.; Dujardin, E.; Cavalier, A.; Moreac, A.; Valéry, C.; Marchi-Artzner, V.; Weiss, T.; Renault, A.; Paternoster, M.; Artzner, F. *Nat. Mater.* **2007**, *6*, 434. (b) Tan, B.; Lehmler, H. J.; Vyas, S. M.; Knutson, B. L.; Rankin, S. E. *Adv. Mater.* **2005**, *17*, 2368. (c) Tan, B.; Vyas, S. M.; Lehmler, H. J.; Knutson, B. L.; Rankin, S. E. *Adv. Funct. Mater.* **2007**, *17*, 2500. (d) Wang, H.; Wang, Y.; Zhou, X.; Zhou, L.; Tang, J.; Lei, J.; Yu, C. Z. *Adv. Funct. Mater.* **2007**, *17*, 613.

(2) (a) Chen, H.; He, J. *J. Colloid Interface Sci.* **2007**, *316*, 211. (b) Yang, M.; Ma, J.; Zhang, C.; Yang, Z. Z.; Lu, Y. F. *Angew. Chem., Int. Ed.* **2005**, *44*, 6727. (c) Tan, B.; Lehmler, H. J.; Vyas, S. M.; Knutson, B. L.; Rankin, S. E. *Chem. Mater.* **2005**, *17*, 916. (d) Yu, M.; Wang, H.; Zhou, X.; Yuan, P.; Yu, C. Z. *J. Am. Chem. Soc.* **2007**, *129*, 14576.

(3) (a) Dähne, L.; Leporatti, S.; Donath, E.; Möhwald, H. *J. Am. Chem. Soc.* **2001**, *123*, 5431. (b) Ibarz, G.; Dähne, L.; Donath, E.; Möhwald, H. *Adv. Mater.* **2001**, *13*, 1324. (c) Tang, J.; Zhou, X.; Zhao, D.; Lu, G.; Zou, J.; Yu, C. Z. *J. Am. Chem. Soc.* **2007**, *129*, 9044.

(4) (a) He, J.; Chen, H.; Zhang, L. *Prog. Chem.* **2007**, *19*, 1488. (b) Arnal, P. M.; Weidenthaler, C.; Schüth, F. *Chem. Mater.* **2006**, *18*, 2733. (c) Ji, X. L.; Hu, Q. Y.; Hampsey, J. E.; Qiu, X. P.; Gao, L. X.; He, J. B.; Lu, Y. F. *Chem. Mater.* **2006**, *18*, 2265.

(5) (a) Lvov, Y.; Antipov, A. A.; Mamedov, A.; Möhwald, H.; Sukhorukov, G. B. *Nano Lett.* **2001**, *1*, 125. (b) Gao, C.; Donath, E.; Möhwald, H.; Shen, J. *Angew. Chem., Int. Ed.* **2002**, *41*, 3789.

(6) (a) Xu, A.; Yu, Q.; Dong, W.; Antonietti, M.; Cölfen, H. *Adv. Mater.* **2005**, *17*, 2217. (b) Sanchez, C.; Arribart, H.; Madeleine, M.; Guille, G. *Nat. Mater.* **2005**, *4*, 277.

(7) Lu, A.; Schüth, F. *Adv. Mater.* **2006**, *18*, 1793.

(8) Titirici, M.; Thomas, A.; Antonietti, M. *Adv. Funct. Mater.* **2007**, *17*, 1010.

(9) Mal, N. K.; Fujiwara, M.; Tanaka, Y. *Nature* **2003**, *421*, 350.

(10) Jiang, X. M.; Brinker, C. J. *J. Am. Chem. Soc.* **2006**, *128*, 4512.

(11) (a) Zhu, Y. F.; Shi, J. L.; Shen, W. H.; Dong, X. P.; Feng, J. W.; Ruan, M. L.; Li, Y. S. *Angew. Chem., Int. Ed.* **2005**, *44*, 5083. (b) Kreilgaard, M. *Adv. Drug Delivery Rev.* **2002**, *54*, 77.

(12) Liu, N. G.; Dunphy, D. R.; Atanassov, P.; Bunge, S. D.; Chen, Z.; López, G. P.; Boyle, T. J.; Brinker, C. J. *Nano Lett.* **2004**, *4*, 551.

(13) Torney, F.; Trewyn, B. G.; Lin, V. S. Y.; Wang, K. *Nat. Nanotechnol.* **2007**, *2*, 295.

(14) Sharma, K. K.; Asefa, T. *Angew. Chem., Int. Ed.* **2007**, *46*, 2879.

(15) Caruso, F.; Caruso, R. A.; Möhwald, H. *Science* **1998**, *282*, 1111.

(16) (a) Suárez, F. J.; Sevilla, M.; Álvarez, S.; Valdés-solis, T.; Fuertes, A. B. *Chem. Mater* **2007**, *19*, 3096. (b) Wu, X.; Tian, Y.; Cui, Y.; Wei, L.; Wang, Q.; Chen, Y. *J. Phys. Chem. C* **2007**, *111*, 9704.

(17) Yang, Z. Z.; Niu, Z.; Lu, Y.; Hu, Z.; Han, C. C. *Angew. Chem., Int. Ed.* **2003**, *42*, 1943.

(18) Khanal, A.; Inoue, Y.; Yada, M.; Nakashima, K. *J. Am. Chem. Soc.* **2007**, *129*, 1534.

(19) Djojoputro, H.; Zhou, X. F.; Qiao, S. Z.; Wang, L. Z.; Yu, C. Z.; Lu, G. Q. *J. Am. Chem. Soc.* **2006**, *128*, 6320.

(20) Wang, J.; Xiao, Q.; Zhou, H.; Sun, P.; Yuan, Z.; Li, B.; Ding, D.; Shi, A.; Chen, T. *Adv. Mater.* **2006**, *18*, 3284.

(21) (a) Liu, J.; Li, C.; Yang, Q.; Yang, J.; Li, C. *Langmuir* **2007**, *23*, 7255. (b) Zhang, H.; Wu, J.; Zhou, L.; Zhang, D.; Qi, L. *Langmuir* **2007**, *23*, 1107.

10.1021/cm801411y CCC: $40.75
Published on Web 09/03/2008

Chart 1. Molecular Structures of Ethyl Ether (a) and 2-Ethoxyethanol (b)

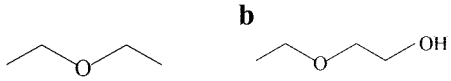

Self-assembly at the dynamic oil−water interface has long been attracting much attention. For example, oleic acid, kerosene, hexane, and trimethylbenzene have been used as both cosolvent and template (droplets) to prepare porous particles and capsules.[19–26] This synthetic strategy, however, involves complex steps that include the removal of the high boiling point emulsion template by either calcination or washing with organic solvents (e.g., acetone and toluene). In the present work, we have successfully fabricated novel silica nanocapsules by dynamic self-assembly at the oil−water interface. Unlike the above emulsion-templating methods using cosolvents of high boiling points, a novel process was developed, in which low boiling point ethyl ether was employed as the cosolvent and template. Silica nanocapsules were obtained eventually by simple gasification of the template. As a control, 2-ethoxyethanol, which only has a small difference in its molecular structure from ethyl ether (see Chart 1), was also used. Instead of silica nanocapsules, silica nanospheres with weakly ordered pores were obtained. Although systematical research on the preparation of porous silica spheres by addition of various alcohols had been reported,[27] the current work studied the effects of varied ethers by considering 2-ethoxyethanol as an ether. We further explored the possibilities of in situ encapsulation of hydrophobic organic molecules by the current approach and their applications in controlled release in aqueous media. To our best knowledge, no reports have been released yet on such an approach to the preparation of silica nanocapsules by ready gasification of the template.

Experimental Section

Materials. Cetyltrimethylammonium bromide (CTAB) (≥99%), ammonia solution (NH_4OH) (25−28%), and ethyl ether (≥99.5%) were obtained from Beijing Chemical Reagent Co. 2-Ethoxyethanol (≥99.5%) was purchased from Sinopharm Chemical Reagent Co. Tetraethoxysilane (TEOS) (99.9%) and pyrene (99%) were purchased from Alfa Aesar. All chemicals were analytic grade and were used without further purification. Pure water used in all experiments had a resistivity of 18.2 MΩ·cm and was obtained from a Milli-Q system (Millipore).

Preparation of Silica Nanocapsules. The silica nanocapsules were synthesized by using CTAB as the modifier (surfactant and porogen) and ethyl ether as the cosolvent. In a typical procedure, 0.5 g of CTAB was dissolved in 70 mL of H_2O. After 0.5 mL of ammonia solution (25∼28%) and 20−50 mL of ethyl ether were added, the mixture was vigorously stirred in a closed vessel at room temperature for 30 min. To the mixture was dripped 2.5 mL of TEOS, and the resulting mixture was vigorously stirred for 24 h. A white precipitate was obtained, filtered, washed with pure water, and dried at 60 °C. CTAB and other organic components were removed by calcination in air at 550 °C for 5 h. When the molar ratios of ethyl ether to CTAB were 141 (20 mL of ethyl ether to 0.5 g of CTAB) and 353 (50 mL of ethyl ether to 0.5 g of CTAB), the prepared silica nanocapsules were named as sample A and sample B, respectively. The yields of silica nanocapsules were ca. 80%.

Preparation of Porous Silica Nanospheres. The silica nanospheres were synthesized by using CTAB as the porogen and 2-ethoxyethanol as the cosolvent. In a typical procedure, 0.5 g of CTAB was dissolved in 70 mL of H_2O, followed by addition of 0.5 mL of ammonia solution (25−28%) and 25−50 mL of 2-ethoxyethanol. After 2.5 mL of TEOS was added to the solution, the mixture was vigorously stirred in a closed vessel for 24 h. A white precipitate was obtained, filtered, washed with pure water, and dried at 60 °C. CTAB and other organic components were removed by calcination in air at 550 °C for 5 h. When the molar ratios of 2-ethoxyethanol to CTAB were 188 (25 mL of 2-ethoxyethanol to 0.5 g of CTAB) and 376 (50 mL of 2-ethoxyethanol to 0.5 g of CTAB), the prepared porous silica nanospheres were named as sample C and sample D, respectively. The yields of porous silica nanospheres were above 90%.

Encapsulation of Fluorescent Pyrene Molecules into Silica Nanocapsules. Dyes such as pyrene could be readily encapsulated into the silica nanocapsules simply by dissolving pyrene in ethyl ether. In a typical procedure, 0.25 g of CTAB was dissolved in 35 mL of H_2O, followed by addition of 0.25 mL of ammonia solution (25−28%) and 20 mL of ethyl ether that contained 0.2 g of pyrene. After 2.0 mL of TEOS was added to the solution, the mixture was vigorously stirred in a closed vessel for 24 h. A white precipitate was obtained, filtered, washed with pure water, and dried at 60 °C. To estimate the weight percentage of encapsulated pyrene, we carried out two parallel experiments with and without addition of pyrene into the reaction mixture. The products were treated under identical conditions, such as a filtration, washing, and drying process. The weight of encapsulated pyrene was estimated from the weight difference of the dried products. The parallel experiments were repeated twice, and the mean value was calculated to be ca. 10% (±2.5%).[28] Finally, 0.05 g of the as-synthesized product was redispersed in 50 mL of pure water under magnetic stirring. A 2−3 mL sample of the suspension was subjected to photoluminescence measurements, and 0.5−1.0 mL of the suspension was diluted by 2 mL of pure water and subjected to UV−vis absorption measurements.

Controlled Release Experiments. Briefly, 0.05 g of pyrene-encapsulated silica nanocapsules was dispersed in 100 mL of pure water under magnetic stirring. A 2.0 mL sample of the mixture was extracted with a syringe at given time intervals for analysis. After removal of the dye-encapsulated nanocapsules by centrifuga-

(22) (a) Chen, H.; He, J. *Chem. Lett.* **2007**, *36*, 174. (b) Chen, H.; He, J.; Zhang, C.; He, H. *J. Phys. Chem. C* **2007**, *111*, 18033. (c) Cheng, X.; Liu, S.; Lu, L.; Sui, X.; Meynen, V.; Cool, P.; Vansant, E. F.; Jiang, J. *Microporous Mesoporous Mater.* **2007**, *98*, 41.
(23) (a) Hubert, D. H. W.; Coombs, N.; Lough, A.; Ozin, G. A. *Nature* **1995**, *378*, 47. (b) Hou, Q.; Leon, R.; Petroff, P. M.; Stucky, G. D. *Science* **1995**, *268*, 1324.
(24) Li, W.; Sha, X.; Dong, W.; Wang, Z. *Chem. Commun.* **2002**, 2434.
(25) Sun, Q. Y.; Kooyman, P. J.; Grossmann, J. G.; Bomans, P. H. H.; Frederik, P. M.; Magusin, P. C. M. M.; Beelen, T. P. M.; van Santen, R. A.; Sommerdijk, N. A. J. M. *Adv. Mater.* **2003**, *15*, 1097.
(26) Fujiwara, M.; Shiokawa, K.; Sakakura, I.; Nakahara, Y. *Nano Lett.* **2006**, *6*, 2925.
(27) (a) Lebedev, O. I.; van Tendeloo, G.; Collart, O.; Cool, P.; Vansant, E. F. *Solid State Sci.* **2004**, *6*, 489. (b) Grün, M.; Latter, I.; Unger, K. K. *Adv. Mater.* **1997**, *9*, 254. (c) Pauwels, B.; van Tendeloo, G.; Thoelen, C.; van Rhijn, W.; Jacobs, P. A. *Adv. Mater.* **2001**, *13*, 1317. (d) Nooney, R. I.; Thirunavukkarasu, D.; Chen, Y.; Josephs, R.; Ostafin, A. E. *Chem. Mater.* **2002**, *14*, 4721. (e) Liu, S.; Cool, P.; Collart, O.; van Der Voort, P.; Vansant, E. F.; Lebedev, O. I.; van Tendeloo, G.; Jiang, M. *J. Phys. Chem. B* **2003**, *107*, 10405.

(28) Equation: weight percentage of pyrene (%) = $100(W_1 - W_0)/W_1$ (where W_1 (g) is the weight of the sample prepared by adding pyrene into the reaction solution and W_0 (g) is the weight of the sample prepared without adding pyrene into the reaction solution).

Scheme 1. Illustration of the Synthetic Procedures of Silica Nanocapsules and Porous Silica Nanospheres

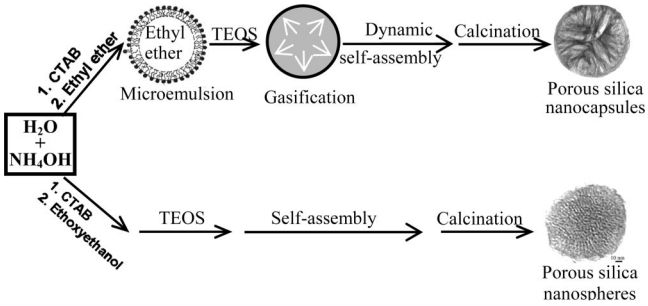

tion (12 000 rpm, 2 min), the extracted mixture was analyzed by UV−vis spectroscopy. All measurements were performed in triplicate.

Characterization. Small-angle X-ray diffraction (XRD) patterns of the as-prepared products were recorded on a Holand PANalytical X'Pert PRO MPD X-ray diffractometer using Cu Kα radiation (λ = 0.1542 nm) operated at 40 kV and 40 mA. Scanning electron microscopy (SEM) observations and energy dispersive spectroscopy (EDS) measurements were carried out on a Hitachi S-4300 field emission scanning electron microscope. All the samples were sputtered with gold before observations. For transmission electron microscopy (TEM) observations, powder samples were added onto carbon-coated copper grids and observed on a JEOL JEM-200CX transmission electron microscope at an acceleration voltage of 150 kV. UV−vis absorption spectra of the nanocapsules containing pyrene (dispersed in water) were recorded on a TU-1901 spectrophotometer (Beijing Purkinje General Instrument Co). Photoluminescence (PL) spectra were recorded on a Hitachi F-4500 fluorometer using an excitation wavelength of 330 nm. The mean diameters of silica nanocapsules and porous nanospheres were determined by randomly sampling over 100 particles, followed by analysis with SigmaPlot 2001. Nitrogen adsorption−desorption measurements were performed on a Quantachrome NOVA 4200e surface area analyzer at −196 °C using the volumetric method. The as-prepared SiO_2 products were dried at 150 °C before analysis. The Brunauer−Emmett−Teller (BET) specific surface areas were calculated by using adsorption data in $P/P_0 = 0.04-0.20$ (six points collected). Pore size distributions were estimated from adsorption branches of the isotherms by using the Barrett, Joyner, and Halenda (BJH) method. Pore volumes were determined from the amounts of N_2 adsorbed at the single point of $P/P_0 = 0.98$.

Results and Discussion

Preparation and Characterization of Porous Silica Nanocapsules and Nanospheres. The synthetic procedures employed are schematically illustrated in Scheme 1. The silica nanocapsules were synthesized by using CTAB as the modifier (surfactant and porogen) and ethyl ether as the cosolvent. As a control, 2-ethoxyethanol, which only has a small difference in its molecular structure from ethyl ether (see Chart 1) was also used. Instead of silica nanocapsules, silica nanospheres with weakly ordered pores were obtained.

A white powder (sample A) was obtained by mixing water, NH_4OH, CTAB, ethyl ether, and TEOS followed by calcination (see the Experimental Section for details). It was observed by SEM and TEM. Typical SEM and TEM images of the white powder are shown in Figure 1. Clearly, the white powder consists of spherical nanoparticles (Figure 1a). The mean diameter of the spherical nanoparticles was estimated to be ca. 120 nm. The corresponding EDS (inset in Figure 1a) showed the presence of Si and O elements, indicating that the spherical nanoparticle was composed of silica. Crackles were noticed on the surface of the spherical nanoparticles, as pointed out by dark arrows in Figure 1b. Very interesting, these spherical particles have a hollow nature, as revealed both by an opening of a particle (Figure 1b, pointed out by a white arrow) and by the contrast between the dark edge and pale center (Figure 1c). Shells of these nanocapsules have a thickness of ca. 20 nm. At higher magnifications (Figure 1d), it can be seen that the shells are in fact porous. From Figure 1d, the pore sizes were estimated to be 2−5 nm. However, reliable determination of the pore size may be obtained from nitrogen sorption analysis, as discussed later. It is noteworthy that pleats can be found clearly in Figure 1c. To clarify whether the pleats of silica nanocapsules formed before or after calcination, the products before calcination were also observed by TEM. Figure 2 shows typical TEM images of silica nanocapsules before (Figure 2a) and after (Figure 2b) calcination at 550 °C. Clearly, the pleats of silica nanocapsules had already formed before calcination rather than during calcination (Figure 2a). In fact, it was noted that ethyl ether flew down along the inner wall of the closed reaction vessel during the sol−gel

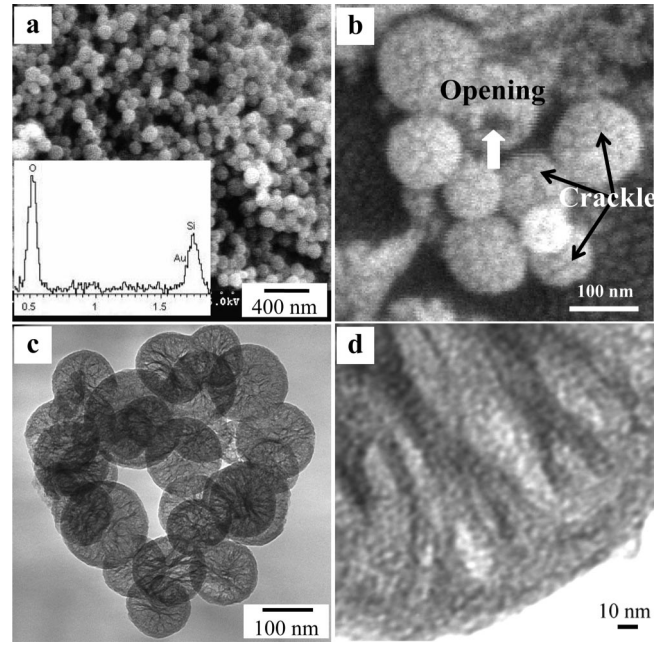

Figure 1. SEM (a, b) and TEM (c, d) images of calcined silica nanocapsules of sample A. The inset in (a) is the corresponding EDS result.

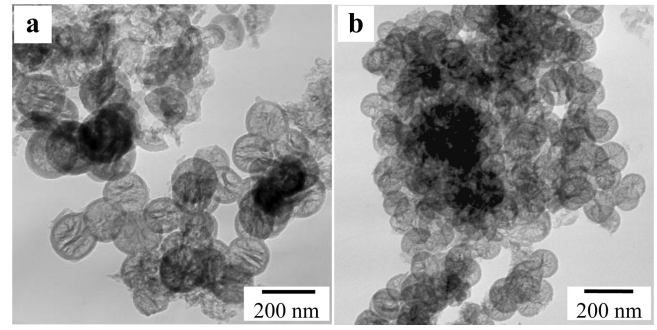

Figure 2. TEM images of silica nanocapsules of sample A before (a) and after (b) calcination at 550 °C.

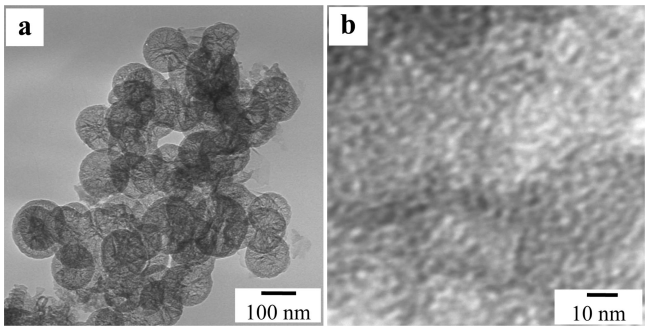

Figure 3. TEM images at low (a) and high (b) magnifications of calcined silica nanocapsules of sample B.

process of TEOS, and when the vessel was opened, ethyl ether evaporated out of the vessel. Thus, the pleats on the silica nanocapsules might result from heterogeneous gasification of ethyl ether (dynamic template) and simultaneous self-assembly of condensed silica. Subsequent calcination at 550 °C for 5 h did not change the morphology of the silica nanocapsules (Figure 2b), indicating that the pleats of the silica nanocapsules had high thermal stability, though the calcination step induced a slight shrinkage of the silica nanocapsules.

To investigate the effect of the molar ratio of the emulsion template (i.e., ethyl ether) to CTAB on the formation of silica nanocapsules, a series of comparative experiments were carried out. In the absence of ethyl ether under otherwise identical conditions, only irregular silica aggregates were obtained. Figure 3 shows TEM images of sample B obtained when the molar ratio was 353. Compared with those of sample A (the molar ratio was 141), the particle size, shell thickness, and surface morphology of the silica nanocapsules did not change much (Figures 1 and 3).[29] The pore structures of sample B (Figure 3b), however, became more ordered than those of sample A (Figure 1d).

When 2-ethoxyethanol was used instead of ethyl ether under otherwise identical conditions, a white powder (sample C) was also obtained by calcination at 550 °C. Figure 4 shows typical SEM and TEM images of the white powder. Clearly, it also consisted of spherical particles (Figure 4a). The diameters of these nanospheres were 40−90 nm. The corresponding EDS spectrum (inset in Figure 4a) showed the presence of Si and O elements, indicating that the nanosphere was composed of silica. The nanospheres had crackles (ca. 6 nm) on their bumpy surface, as pointed out by arrows in Figure 4b. Parts c and d of Figure 4 show TEM images of the nanospheres. Apparently, channel-like pores ca. 4 nm in width (as pointed out by arrows) were present inside the nanospheres (Figure 4d). A series of comparative experiments were also carried out by changing the molar ratio of 2-ethoxyethanol to CTAB. Figure 5 shows TEM images of sample D obtained when the molar ratio was 376 under otherwise identical conditions. The nanospheres obtained (Figure 5a) had a smoother surface, larger particle size (ca. 300 nm), and more uniform particle size than those of sample C (Figure 4). Ordered pore structures ca. 3 nm in width were also observed (Figure 5b).

(29) Han, Y.; Ying, J. Y. *Angew. Chem., Int. Ed.* **2005**, *44*, 288.

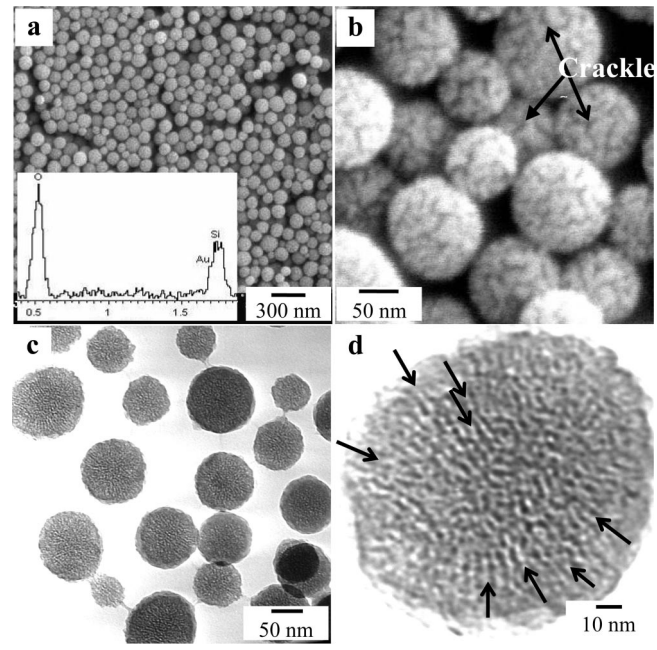

Figure 4. SEM (a, b) and TEM (c, d) images of calcined porous silica nanospheres of sample C. The inset in (a) is the corresponding EDS result.

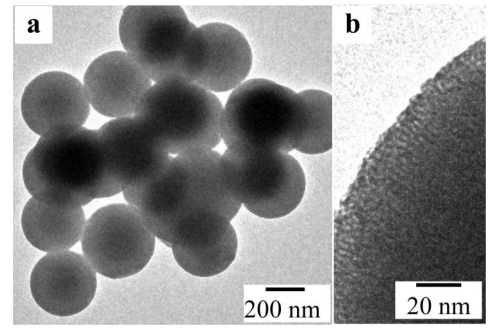

Figure 5. TEM images at low (a) and high (b) magnifications of calcined porous silica nanospheres of sample D.

Small-angle XRD patterns of the calcined samples are shown in Figure 6. The nanocapsules of sample A showed no reflection (Figure 6a), and those of sample B showed a very broad peak at $2\theta = 2.37°$ with a d spacing of 3.6 nm (Figure 6b). The porous nanospheres of sample C showed a slightly narrower peak at $2\theta = 2.31°$ with a d spacing of 3.8 nm (Figure 6c), and those of sample D showed an even narrower and stronger peak at $2\theta = 2.13°$ with a d spacing of 4.2 nm (Figure 6d). Although the difference was small, these results may suggest that more ordered porous structures of silica nanocapsules and porous nanospheres had been produced by an increase of the molar ratio of cosolvent to surfactant, agreeing well with the previous report that the pore diameter of porous silica spheres could be tailed by changing the molar ratio of cosolvent (trimethylbenzene) to surfactant ($EO_xPO_yEO_x$).[29] The more ordered structure of porous silica nanospheres than that of silica nanocapsules also suggested that 2-ethoxyethanol might be more easily assembled with CTAB than ethyl ether. In contrast, irregular aggregates that showed no reflection (Figure 6e) were obtained by adding neither ethyl ether nor 2-ethoxyethanol, indicating that the structure of the aggregates was disordered.

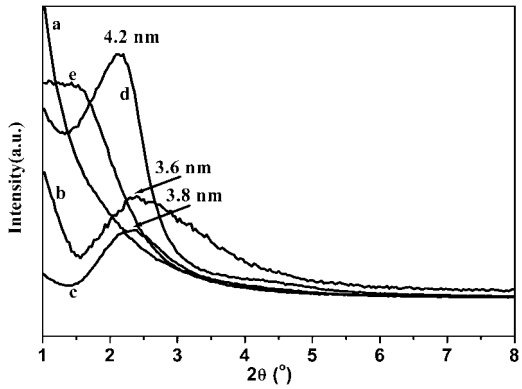

Figure 6. XRD patterns of samples A (a), B (b), C (c), and D (d) and irregular aggregates (e) prepared in the absence of cosolvent.

Nitrogen adsorption−desorption measurements of silica nanocapsules (Figure 7a,c) and porous silica nanospheres (Figure 7e,g) all revealed a typical adsorption−desorption isotherm, indicating the presence of both micropores and mesopores.[30] A sharp increase in nitrogen uptake in a range of relative pressure (P/P_0) of 0.9−1.0 should correspond to the voids formed between silica nanoparticles.[29] Both silica nanocapsules and porous silica nanospheres had typical H3 adsorption−desorption hysteresis loops, indicating that they had slit-shaped pores,[30] in agreement with the results drawn from Figures 1 and 4. Interestingly, the silica nanocapsules had larger hysteresis loops than the porous nanospheres.[1c] Similar results were noticed from their pore size distributions (Figure 7b,d,f,h). Clearly, the silica nanocapsules had a wider size distribution than the porous silica nanospheres.

More detailed information was obtained by surface and small-angle XRD analyses of the silica nanostructures. As shown in Table 1, when the molar ratio of ethyl ether to CTAB was increased, the *d* spacing of silica nanocapsules changed from 0 (sample A) to 3.6 nm (sample B). Meanwhile, their BET specific surface area and single-point total pore volume at $P/P_0 = 0.98$ increased from 710 m^2/g and 0.98 cm^3/g (sample A) to 784 m^2/g and 1.17 cm^3/g (sample B), respectively. The pore size distributions of both sample A (Figure 7b) and sample B (Figure 7d) showed wide distributions and only a weak peak at 3.7 nm and a strong weak at 3.8 nm. Similarly, the *d* spacing of porous silica nanospheres changed from 3.8 nm (sample C) to 4.2 nm (sample D), and their BET specific surface area increased from 773 m^2/g (sample C) to 947 m^2/g (sample D). The single-point total pore volume at $P/P_0 = 0.98$ of sample C (0.89 cm^3/g) was also lower than that of sample D (1.26 cm^3/g). The pore size distribution of sample C showed a strong peak at 2.5 nm (Figure 7f). In contrast, sample D showed a stronger peak at 2.4 nm (Figure 7h). It is clear that the cosolvents added to the surfactant solutions could increase the porosity of the products significantly and result in concomitant increases of the *d* spacing and pore

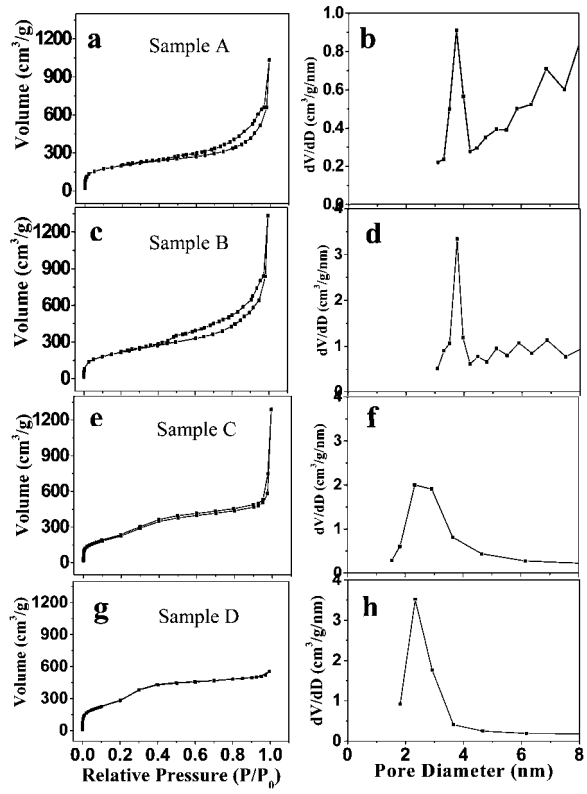

Figure 7. Nitrogen adsorption−desorption isotherms of silica nanocapsules (a, c) and porous silica nanospheres (e, g) and pore size distributions of silica nanocapsules (b, d) and porous silica nanospheres (f, h).

diameter.[29,31] Therefore, the current synthetic protocol could give much more facile control over the morphology, pore order, and BET surface area of silica nanostructures.[29]

Discussion of the Formation of Porous Silica Nanocapsules and Nanospheres. Although the molecular structures of ethyl ether and 2-ethoxyethanol only have a small difference, two completely different silica nanostructures were obtained by using them as the cosolvent. The large difference of these two molecules in boiling point may contribute to the structural difference. The hydrophobic property of ethyl ether and the hydrophilic property of 2-ethoxyethanol may also play critical roles in leading to such a significant difference.

A transparent, colorless microemulsion system is formed after mixing water, NH_4OH, CTAB, and ethyl ether under vigorous stirring. After TEOS is added to the mixture, both condensation of the silica precursor and self-assembly of silica species simultaneously occur on the surface of nanodroplets. Meanwhile, because of the exothermic hydrolysis of TEOS, ethyl ether (boiling point 34 °C) continuously gasified, escaped from the unstable emulsion, and passed through the shells of condensed silica, forming nanochannels. More condensed silica species self-assembled around the channels with the assistance of CTAB. Therefore, some pleats and crackles formed on the shells. The spherical ether templates finally gasified completely, leaving nanohollows.

(30) (a) Sing, K. S. W.; Everett, D. H.; Haul, R. A. W.; Moscou, L.; Piertti, R. A.; Rouquèrol, J.; Siemieniewska, T. *Pure Appl. Chem.* **1985**, *57*, 603. (b) Lowell, S.; Shields, J. E. *Powder Surface Area and Porosity*; Chapman and Hall: New York, 1991.

(31) (a) Beck, J. S.; Vartuli, J. C.; Roth, W. J.; Leonowicz, M. E.; Kresge, C. T.; Schmitt, K. D.; Chu, C. T.-W.; Olson, D. H.; Sheppard, E. W.; Mccullen, S. B.; Higgins, J. B.; Schlenkert, J. L. *J. Am. Chem. Soc.* **1992**, *114*, 10834. (b) Kresge, C. T.; Leonwicz, M. E.; Roth, W. J.; Vartuli, J. C.; Beck, J. S. *Nature* **1992**, *359*, 710.

Table 1. Summary of the Morphologies and Physicochemical Properties of Silica Nanostructures Synthesized Using Varied Molar Ratios (*X*) of Ethyl Ether or 2-Ethoxyethanol to CTAB

cosolvent	*X*	morphology	*d* spacing (nm)	pore size distribution[a] (nm)	surface area [b] (m^2/g)	pore volume[c] (cm^3/g)
ethyl ether	141	capsules		3.7	710	0.98
ethyl ether	353	capsules	3.6	3.8	784	1.17
2-ethoxyethanol	188	porous spheres	3.8	2.5	773	0.89
2-ethoxyethanol	376	porous spheres	4.2	2.4	947	1.26

[a] Calculated from the N_2 adsorption branch using the BJH method. [b] Calculated from the N_2 adsorption branch using the BET method. [c] Estimated from the single-point amount adsorbed at $P/P_0 = 0.98$.

The process exerts a dynamic control and offers a unique opportunity to generate nanocapsules with hierarchically structured shells.[32] In the synthesis, CTAB plays a critical role in stabilizing the nanodroplets and thus in the formation of silica nanocapsules. Without the addition of CTAB, the mixture was opaque, and the sol−gel process of TEOS did not happen even if the solution was kept overnight under vigorous stirring. After the stirring of the mixture was stopped, it became clear, and two separated transparent phases were clearly seen, although ethyl ether is slightly dissolvable in water (ca. 8 g/100 mL of water). It again pointed out the important role of ethyl ether as the template and that of CTAB in stabilizing the dynamic template in the formation of nanocapsules. Following the above speculation, silica nanocapsules with pleats would result from a dynamic cross-coupling of two processes: a dynamical gasification of template (i.e., ethyl ether) and a stabilizing process of condensation and self-assembly. This "dynamical template" concept could be further generalized as a rational preparation scheme for materials with well-defined multiscale architectures.[1a,6,20] Thus, both ethyl ether and CTAB play key roles as dynamical template and stabilizing agent in the formation of silica nanocapsules. When 2-ethoxyethanol was used as the cosolvent, porous nanospheres were obtained.[33] 2-Ethoxyethanol is expected to function both as a solvent and as a cosurfactant.[23,27] Clearly, the current results suggested a synergistic role of CTAB (surfactant) and 2-ethoxyethanol (cosurfactant) in determining the morphology and pore structure of porous silica nanospheres.[27,29,34]

Encapsulation in Situ of Organic Dye Molecules and Their Controlled Release. The hollow nature of the silica nanocapsules makes them particularly suitable as nanocontainers for applications such as drug delivery, controlled release, etc. Previously, drugs or dyes were incorporated in porous spheres usually by postadsorption,[8–10] and few were encapsulated in situ during the synthesis of hollow spheres.[35] As we know, most drug molecules are hydrophobic and soluble in organic solvents, such as ethyl ether. Thus, it is very interesting to explore the possibilities of in situ encapsulation of organic molecules, such as drugs and dyes. For better visualization, we chose pyrene, a hydrophobic fluorescent dye, to investigate the container-type functionality

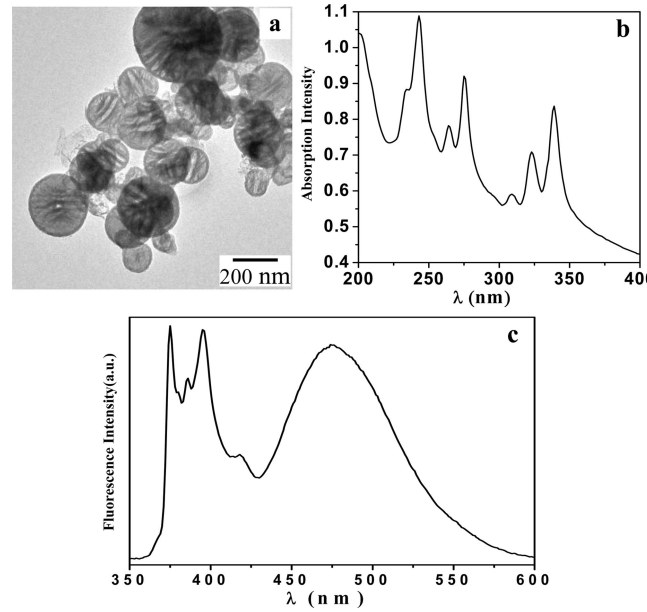

Figure 8. TEM image (a), UV−vis absorption spectrum (b), and fluorescence spectrum (c) of pyrene-encapsulated silica nanocapsules.

Scheme 2. Schematic Illustration of Pyrene Encapsulation and Release: (a) Emulsion System with Reactants, (b) Formation of Pyrene-Encapsulated Silica Nanocapsules, (c) Release of Pyrene into Aqueous Media

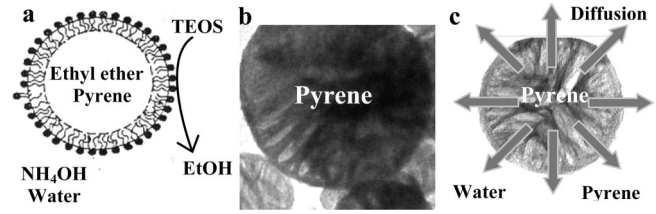

of the silica nanocapsules. As shown in Scheme 2a, pyrene was initially dissolved in ethyl ether in the emulsion droplet and was encapsulated in situ into silica nanocapsules during their formation (Scheme 2a). The pyrene-encapsulated silica nanocapsules were prepared (Scheme 2b). No significant changes in the morphology of the silica nanocapsules were observed after immobilization of the dye molecules (Figure 8a). However, the particle size was not as uniform as those obtained without adding the dye molecules (see Figures 1c and 8a). Figure 8b shows the UV−vis absorption spectrum of a diluted dispersion of pyrene-encapsulated silica nanocapsules. Clearly, only the absorption peaks of pyrene monomer were observed in the range of 220−350 nm.[36]

(32) Kim, I.; Lee, K. *J. Appl. Polym. Sci.* **2003**, *89*, 2562.
(33) Brinker, C. J.; Lu, Y.; Sellinger, A.; Fan, H. *Adv. Mater.* **1999**, *11*, 579.
(34) (a) Jagannathan, N. R.; Venkateswaran, K.; Herring, F. G.; Patey, G. N.; Walker, D. C. *J. Phys. Chem.* **1987**, *91*, 4553. (b) Tan, B.; Rankin, S. E. *J. Phys. Chem. B* **2004**, *108*, 20122.
(35) Botterhuis, N. E.; Sun, Q.; Magusin, P. C. M. M.; van Santen, R. A.; Sommerdijk, N. A. J. M. *Chem.—Eur. J.* **2006**, *12*, 1448.
(36) (a) Cho, S. Y.; Allcock, H. R. *Macromolecules* **2007**, *40*, 3115. (b) Zhang, X.; Zhang, X.; Shi, W.; Meng, X.; Lee, C.; Lee, S. *J. Phys. Chem. B* **2005**, *109*, 18777.

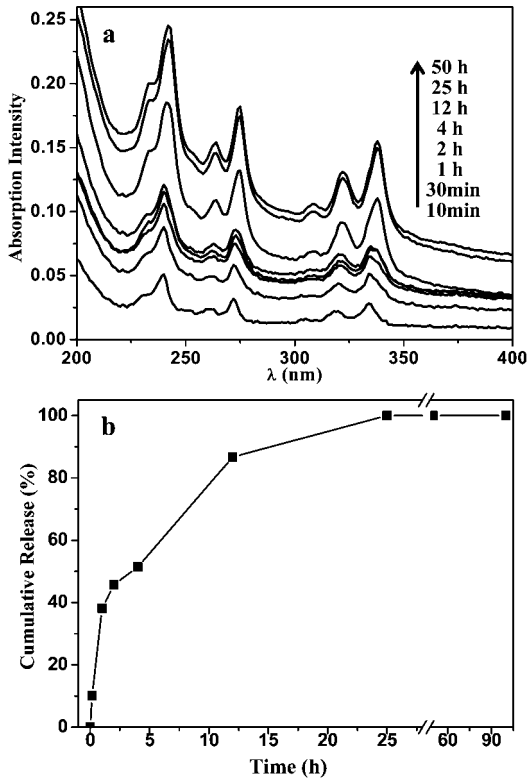

Figure 9. (a) UV−vis spectra at different times of the aqueous media in which pyrene was released from pyrene-encapsulated silica nanocapsules and (b) corresponding controlled release kinetics of pyrene-encapsulated silica nanocapsules.

Figure 8c shows their fluorescence emission spectrum. Apparently, the dispersion exhibited the characteristic emissions (370−410 nm) of the pyrene monomer.[36] In addition, the emission of aggregation modes of pyrene molecules was also recorded at 476 nm.[36b] Other hydrophobic organic molecules, such as dyes, drugs, etc., may also be in situ encapsulated into silica nanocapsules by the current approach.

Controlled release of pyrene was examined by redispersing the pyrene-encapsulated silica nanocapsules in water (Scheme 2c). The releasing process was monitored by following the absorption change of the aqueous media in the range of 200−400 nm after removal of the silica nanocapsules. As shown in Figure 9a, pyrene was doubtlessly released into the aqueous media. A normalized cumulative release was estimated according to the following equation:

$$\text{cumulative release (\%)} = \text{Abs}_t/\text{Abs}_{\max} \times 100 \qquad (1)$$

(where $\text{Abs}_{\max}$ is the absorbance of the peak at ca. 240 nm recorded at 25 h, after which the peak intensity no longer changed and Abs_t is the absorbance of the same peak recorded at time t). A kinetic release curve was plotted from Figure 9a by using the absorption of the peak at ca. 240 nm. As shown in Figure 9b, the releasing process initially proceeded relatively fast, and nearly 38% of the pyrene was released into the aqueous media in 1 h. The releasing process gradually slowed and leveled off after 25 h, indicating that the release reached equilibrium. These results indicated that in situ encapsulation and controlled release of organic molecules had been realized. The release proceeded by diffusion of guest molecules into aqueous media through the shells of nanocapsules.[11,35]

Conclusions

In summary, porous silica nanocapsules and silica nanospheres have been successfully fabricated by a novel combination of stabilizing condensation and dynamic self-assembly. When ethyl ether was used as the cosolvent, porous silica nanocapsules were obtained. Ethyl ether not only functioned as a dynamic template for the formation of the nanocapsule, but also played a critical role in the formation of the porous shell by gasification.[37] In contrast, when 2-ethoxyethanol was used, silica porous nanospheres were produced. It is very interesting that the approach using ethyl ether allowed ready in situ encapsulation of organic molecules into silica nanocapsules, and the encapsulated molecules could be released in a controlled way into aqueous media.

There are three implications of the current results. First, the ethyl ether template is readily eliminated by in situ gasification. Compared with previous strategies in which removal of templates for forming hollows was required by either calcination or extraction, no subsequent processes are needed by the current approach. Second, it is possible to fabricate completely different nanostructures by applying simple molecules of small structural differences. Third, organic molecules can be readily encapsulated in situ into silica nanocapsules by the current approaches. As many dyes, drugs, etc. are organic molecules, the current approaches will doubtlessly open many possibilities toward biological and technological applications.

Acknowledgment. This work was supported by the National Natural Science Foundation of China (Grant Nos.10776034 and 20471065), the National Basic Research Program of China (Grant No. 2006CB933000), and the "Hundred Talents Program" of the CAS. We are very grateful to Prof. T. Kunitake for his encouraging discussion.

CM801411Y

(37) Li, H.; Bian, Z.; Zhu, J.; Zhang, D.; Li, G.; Huo, Y.; Li, H.; Lu, Y. *J. Am. Chem. Soc.* **2007**, *129*, 8406.